DOI: 10.1002/ejic.200801168

Single-Crystal Structure Determination and Solid-State NMR Investigations of Lithium Nitridosilicate Li_2SiN_2 Synthesized by a Precursor Approach Employing Amorphous "$Si(CN_2)_2$"

Sandro Pagano,[a] Martin Zeuner,[a] Stephan Hug,[a] and Wolfgang Schnick*[a]

Keywords: Lithium / Silicon / Nitridosilicates / Solid-state structures

Amorphous silicon bis(carbodiimide) "$Si(CN_2)_2$" has been identified as a reactive precursor for the synthesis of nitridosilicates that is specifically useful in the temperature region below 1000 °C. In this context the applicability and reactivity of amorphous "$Si(CN_2)_2$" towards Li_3N in comparison to silicon diimide $Si(NH)_2$ has been studied using high-temperature in situ powder diffraction and DSC measurements. During the current investigation single crystals of Li_2SiN_2 have been obtained and the crystal structure of this Li^+ ion conductor has been determined and refined: [*Pbca*, no. 61, a = 9.907(2), b = 9.907(2), c = 15.014(3) Å, Z = 32, R_1 = 0.038, 1460 data, 142 parameters]. In the solid, Li_2SiN_2 consists of two interpenetrating cristobalite type nets which are made up from hetero-adamantane-like $[Si_4N_6]N_{4/2}$ groups. The eight crystallographically independent Li^+ sites are ordered at room temp. and exhibit coordination numbers 3 to 5. The ^7Li and ^{29}Si solid-state MAS NMR spectra of Li_2SiN_2 are reported.

Introduction

Investigation of nitridosilicates and related compounds (e.g. oxonitridosilicates and SiAlONs) is an emerging and rapidly growing field of research in materials chemistry. This is due to a variety of applications for theses compounds both as structural and functional materials.[1,2] Besides their structural diversity a remarkable thermal, mechanical and chemical stability has been reported.[3,4] Recently, alkaline earth nitridosilicates and oxonitridosilicates have gained attention as host lattices for rare earth-doped luminescent materials in phosphor-converted pc-LEDs.[2,5–8] Commonly, nitridosilicates (e.g. $M_2Si_5N_8$ with M = Ca, Sr, Eu or Ba)[9,10] have been synthesized at high temperatures around 1600 °C starting from the respective metals or oxides and silicon nitride or silicon diimide $[Si(NH)_2]$.[11] At temperatures of 900–1000 °C, decomposition of $Si(NH)_2$ starts with subsequent formation of amorphous silicon nitride. Thus, using reactive $Si(NH)_2$ as a precursor for Si_3N_4, the reaction temperatures can be lowered significantly.[11] Focusing on less stable alkali nitridosilicates, reactive Si/N precursors are advantageous in order to avoid decomposition of the products and/or evaporation of the alkali metal. During our search for reactive Si/N precursors, we have tried to reproduce the synthesis of $Si(CN_2)_2$ reported by Riedel et al.[12] Amorphous silicon bis(carbodiimide) has been synthesized by the reaction of $SiCl_4$ with bis(trimethylsilyl)carbodiimide. The by-product chlorotrimethylsilane was removed by evaporation under vacuum. Calcination of the reaction mixture at 350 °C yields amorphous "$Si(CN_2)_2$" still containing residual methyl groups. The stoichiometric formula as suggested by Riedel et al. $(CH_3)_3Si\text{-}NCN\text{-}[Si_4(NCN)_8]\text{-}Si(CH_3)_3$ is in accordance with our elemental analysis. Crystalline $Si(CN_2)_2$ has been reported to form above 400 °C consisting of 3D-connected $Si(CN_2)_4$ groups building two interpenetrating cristobalite analogous nets.[12] In order to distinguish between crystalline and amorphous $Si(CN_2)_2$, the latter is put into quotation marks. However, we were not able to obtain crystalline and hydrogen free bulk samples of $Si(CN_2)_2$. Nevertheless, amorphous "$Si(CN_2)_2$" turned out to be a promising precursor as silicon nitrides are formed by the release of $(CN)_2$ at elevated temperatures.[12,13] The residual trimethylsilyl-groups could be even advantageous, as nitrogen-bound trimethylsilyl-groups are known to be promising precursors for nitrides.[14] To study the reactivity of "$Si(CN_2)_2$" in comparison to $Si(NH)_2$ we focused on lithium nitridosilicates. In the quasi binary system Li_3N–Si_3N_4, a variety of phases has been reported in the literature (e.g. $LiSi_2N_3$,[15] Li_2SiN_2,[16–18] Li_5SiN_3,[19] Li_8SiN_4, $Li_{18}Si_3N_{10}$[20] and $Li_{21}Si_3N_{11}$[21]). Lithium ion conductivity has been observed and comprehensively studied for Li_2SiN_2 ($\sigma_{400k} = 1.1 \times 10^{-3}\ \Omega^{-1}\ cm^{-1}$) and Li_8SiN_4 ($\sigma_{400k} = 5 \times 10^{-2}\ \Omega^{-1}\ cm^{-1}$).[17,21–23] From a structural point of view lithium nitridosilicates have only been characterized insufficiently and for none of these phases except $LiSi_2N_3$[15] de-

[a] Ludwig-Maximilians-Universität München, Department Chemie und Biochemie,
Butenandtstraße 5–13, 81377 München, Germany
Fax: +49-89-2180-77440
E-mail: wolfgang.schnick@uni-muenchen.de

Supporting information for this article is available on the WWW under http://www.eurjic.org or from the author.

tailed structural data can be found in the literature or in databases. However, with respect to the quasi binary system Li_3N–P_3N_5, nitrides with remarkable structural features (e.g. $Li_{10}P_4N_{10}$[24]) might be accessible in the system Li_3N–Si_3N_4 as well. The structure of $LiSi_2N_3$ was solved from single crystals obtained by the reaction between Li metal and the precursor $Si(NH)_2$. During the current investigations in the quasi binary system Li_3N–Si_3N_4, we found that Li_2SiN_2 is the prevailing product when the synthesis is performed in closed systems and at temperatures between 800 and 1200 °C. For Li_2SiN_2 a synthetic approach has been reported and the crystal structure has been discussed,[16,18] but to the best of our knowledge no detailed information concerning structure analysis nor crystallographic data are available in the literature. In order to characterize this interesting material more deeply that often has been discussed in the context of lithium ion conductivity[21,22] we report on the crystal structure as well as the ^7Li and ^{29}Si solid-state MAS NMR spectra of Li_2SiN_2.

Results and Discussion

Reaction Behavior of "Si(CN$_2$)$_2$"

The reaction between "$Si(CN_2)_2$" and Li_3N was monitored using high-temperature in situ X-ray diffractometry (HT-PXRD) and ex situ DSC measurements. Accordingly, at temperatures above 450 °C Li_2CN_2 is formed causing a broad exothermic DSC signal and yielding the corresponding reflections in the HT-PXRD. A second exothermic event at 600 °C may be attributed to the formation of an amorphous Li/Si/N pre-phase as crystalline Li_2SiN_2 could not be detected below 750 °C. A nitride forming decomposition of the carbodiimide moieties of "$Si(CN_2)_2$" was not observed below 900 °C by Riedel et al.[12,13] Accordingly, we assume, that the carbodiimide moieties at the silicon atoms can be substituted by nitride ions. Thus the reaction mechanism for "$Si(CN_2)_2$" may be described in terms of a metathesis reaction [see Equations (1) and (2)]. In contrast, $Si(NH)_2$ condenses to amorphous Si_3N_4 and the exothermic event detected during DSC measurements at 600 °C can also be attributed to the formation of an amorphous Li/Si/N pre-phase. The HT-PXRD measurements yielded no crystalline phases up to 750 °C for the reaction of $Si(NH)_2$ and Li_3N. In summary, the pseudo-chalcogen CN_2^{2-} is isolobal to NH^{2-} but exhibits a different reaction behavior, which makes it useful for metathesis reactions.

$$\text{"Si(CN}_2\text{)}_2\text{"} + 2Li_3N \rightarrow Li_2SiN_2 + 2Li_2CN_2 \quad (1)$$

$$3Si(NH)_2 + 2Li_3N \rightarrow 3Li_2SiN_2 + 2NH_3 \quad (2)$$

By transferring the results obtained from the DSC measurements to reactions in closed tantalum crucibles, we have found that Li_2SiN_2 is the main product at temperatures from 800 to 1200 °C. The formation of crystalline Li_2SiN_2 starts at 800 °C for both $Si(NH)_2$ and "$Si(CN_2)_2$". Due to the differing reaction mechanisms better crystallinity is observed for "$Si(CN_2)_2$". The best single crystals of Li_2SiN_2 were obtained from the reaction between "$Si(CN_2)_2$" and Li_3N.

In contrast, bulk samples of Li_2SiN_2 for solid-state NMR were synthesized from $Si(NH)_2$ at 1200 °C to obtain a highly crystalline product with no residuals of other Li species (e.g. Li_2CN_2). A PXRD pattern of phase pure Li_2SiN_2 can be found in the Supporting Information. A SEM image of agglomerated bar-like crystallites of Li_2SiN_2 is depicted in Figure 1.

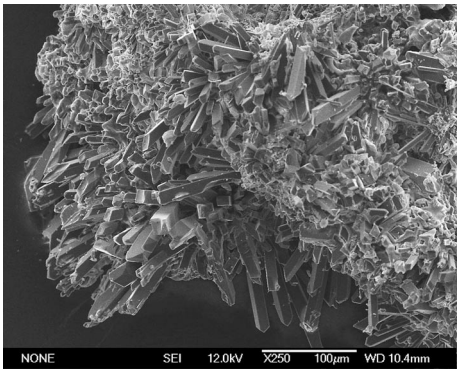

Figure 1. SEM image of Li_2SiN_2.

Crystal Structure of Li$_2$SiN$_2$

In the past few years several attempts have been reported to determine the crystal structure of Li_2SiN_2. In 1993, Hillebrecht et al. obtained single-crystals of Li_2SiN_2 from the reaction between Li_3N and Si at 1227 °C in closed tantalum tubes.[18] The authors observed pseudo-meroedric twinning caused by the pseudo tetragonal unit cell of the compound. The basic structural results of their structure solution are in agreement with our findings. Nevertheless, a detailed report on the crystal structure analysis has not been published in the literature as yet. More than 10 years later, Esmaeilzadeh et al. reported again on the $[SiN_2]^{2-}$ tetrahedron network in Li_2SiN_2, but they were unable to locate unequivocally the positions of the Li^+ ions.[16] This was probably due to the structure solution from powder neutron diffraction data in the tetragonal space group $I4_1acd$. The crystals we obtained from the reaction between $Si(NH)_2$ and Li_3N also exhibited pseudo-meroedric twinning. However, the crystals we selected from the reaction between "$Si(CN_2)_2$" and Li_3N with an identical temperature program showed no twinning at all and were used for the reported structure solution and refinement (see Tables 1, 2, and 3). Li_2SiN_2 crystallizes as colorless needles (Figure 1) in the orthorhombic space group *Pbca*, which has also been suggested by Hillebrecht et al.[18] The asymmetric unit consists of one symmetrically independent $[Si_4N_6]N_{4/2}$ group as well as eight Li^+ ions (Figure 3) and the unit cell is filled up from 32 formula units. The $[SiN_2]^{2-}$ tetrahedron network is built up from super-tetrahedrons (hetero-adamantane groups $[Si_4N_6]N_{4/2}$) forming two interpenetrating cristobalite analogous nets. The two identical, non-connected $[SiN_2]^{2-}$ sub-

structures are related to another by an inversion center. Li_2SiN_2 underlines the large structural variety for nitridosilicates with a molar ration Si/N = 1:2 (e.g. $MSiN_2$; M = Mg, Ca, Sr, Ba).[25] Figure 2 illustrates one branch of the cristobalite analogous net disregarding that each super-tetrahedron is further connected to four neighboring super-tetrahedrons. The formation of adamantane-like structures has not been observed in other nitridosiliactes, but has been reported for the nitridophosphate $Li_{10}P_4N_{10}$.[24]

Table 1. Crystallographic data of Li_2SiN_2.

Formula	Li_2SiN_2
Formula mass [g mol^{-1}]	69.98
Crystal system	orthorhombic
Space group	*Pbca* (no. 61)
Cell parameters [Å]	a = 9.907(2), b = 9.907(2), c = 15.014(3)
Cell volume [10^6 pm^3]	V = 1473.5(5)
Formula units/cell	32
Crystal size [mm]^3	0.10 × 0.09 × 0.08
$\rho_{calcd.}$ [g cm^{-3}]	2.524
μ [mm^{-1}]	0.77
F(000)	1088
Diffractometer	Stoe IPDS
Temperature [K]	295(2)
Radiation, monochromator	Mo-K_α, (λ = 71.073 pm), graphite
Absorption correction	None
θ range [°]	2.71–28.5
Measured reflections	12479
Independent reflections	1865
Observed reflections	1460
Refined parameters	142
GoF	1.026
R indices [$F_o^2 \geq 2\sigma(F_o^2)$]	$R1$ = 0.0381, $wR2$ = 0.0915
R indices (all data)	$R1$ = 0.0525, $wR2$ = 0.0964[a]
Max./min. residual electron density [e Å^{-3}]	0.509/–0.559

[a] $w = [\sigma^2(F_o^2) + (0.0610\ P)^2 + 0.00\ P]^{-1}$ where $P = (F_o^2 + 2\ F_c^2)/3$.

Table 2. Atomic coordinates and equivalent displacement parameters [Å^2] for Li_2SiN_2; all atoms are on Wyckoff position 8*c*.

Atom	x	y	z	U_{eq}/U_{iso}[a]
Li1	0.3992(5)	–0.1520(5)	0.6225(3)	0.0092(9)
Li2	0.6033(5)	0.0613(5)	0.5210(3)	0.0109(9)
Li3	0.8278(5)	–0.1616(5)	0.7282(4)	0.0131(10)
Li4	0.1365(5)	–0.0775(5)	0.5372(3)	0.0113(9)
Li5	0.8620(5)	0.2960(5)	0.6214(4)	0.0135(10)
Li6	0.8088(5)	0.1062(5)	0.7840(4)	0.0132(9)
Li7	0.7921(5)	0.0283(5)	0.6247(3)	0.0108(9)
Li8	0.4566(5)	0.6192(5)	0.6266(4)	0.0154(10)
Si1	0.35840(7)	0.16714(7)	0.55669(5)	0.00347(18)
Si2	0.60895(7)	0.31932(7)	0.55739(5)	0.00303(18)
Si3	0.41375(7)	0.35598(7)	0.69948(5)	0.00315(18)
Si4	0.56649(7)	0.10480(7)	0.68655(5)	0.00328(18)
N1	0.4428(2)	0.0410(2)	0.61512(15)	0.0054(4)
N2	0.2365(2)	0.0894(2)	0.49276(15)	0.0049(4)
N3	0.5318(2)	0.4332(2)	0.62996(15)	0.0050(4)
N4	0.6611(2)	–0.0248(2)	0.73275(15)	0.0041(4)
N5	0.6839(2)	0.1928(2)	0.62174(15)	0.0046(4)
N6	0.2895(2)	0.2813(2)	0.63277(16)	0.0051(4)
N7	0.4933(2)	0.2249(2)	0.76136(16)	0.0050(4)
N8	0.4836(2)	0.2500(2)	0.48796(15)	0.0055(4)

[a] U_{eq} is defined as 1/3 of the trace of the U_{ij} tensors; U_{eq} for Li.

Table 3. Selected interatomic distances [Å] for Li_2SiN_2.

Li1	Li2	2.335(7)	Li5	N5	2.040(5)
Li1	Li3	2.352(7)	Li5	N7	2.300(6)
Li1	Li4	2.994(7)	Li5	N8	2.086(6)
Li1	Li5	2.421(7)	Li6	Li3	2.797(7)
Li1	Li6	3.052(7)	Li6	Li7	2.518(7)
Li1	Li8	2.338(7)	Li6	Li8	2.955(7)
Li1	N1	1.963(5)	Li6	N1	2.116(6)
Li1	N6	1.989(5)	Li6	N4	2.102(6)
Li1	N7	2.379(5)	Li6	N6	2.147(6)
Li1	N8	2.246(5)	Li6	N7	2.278(6)
Li2	Li2	2.463(10)	Li7	Li8	2.648(7)
Li2	Li7	2.455(7)	Li7	N2	2.133(5)
Li2	N1	2.327(5)	Li7	N3	1.985(5)
Li2	N1	2.136(5)	Li7	N4	2.143(5)
Li2	N2	2.189(5)	Li7	N5	1.951(5)
Li2	N5	2.149(5)	Li8	Li4	3.064(7)
Li2	N8	2.269(5)	Li8	N3	1.988(6)
Li3	Li5	2.507(7)	Li8	N7	2.043(6)
Li3	Li7	2.466(7)	Li8	N8	2.233(6)
Li3	N3	2.234(6)	Si1	N1	1.741(2)
Li3	N4	2.137(5)	Si1	N2	1.724(2)
Li3	N5	2.156(6)	Si1	N6	1.746(2)
Li3	N6	2.455(6)	Si1	N8	1.810(2)
Li3	N7	2.157(5)	Si2	N2	1.727(2)
Li4	Li7	2.578(7)	Si2	N3	1.744(2)
Li4	Li8	2.539(7)	Si2	N5	1.748(2)
Li4	N2	2.040(5)	Si2	N8	1.761(2)
Li4	N3	2.175(5)	Si3	N3	1.744(2)
Li4	N6	2.134(6)	Si3	N4	1.726(2)
Li4	N8	2.209(5)	Si3	N6	1.751(2)
Li5	Li7	2.742(7)	Si3	N7	1.781(2)
Li5	Li7	2.762(7)	Si4	N1	1.747(2)
Li5	Li8	2.511(7)	Si4	N4	1.735(2)
Li5	N2	2.402(6)	Si4	N5	1.749(2)
Li5	N4	2.449(6)	Si4	N7	1.790(2)

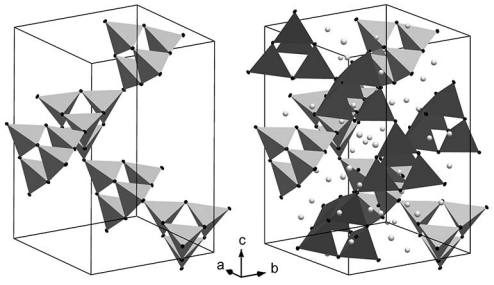

Figure 2. One branch of the $[Si_4N_6]N_{4/2}$ network of Li_2SiN_2 (left). Crystal structure of Li_2SiN_2 (right). [SiN_4] units are depicted as closed gray polyhedrons, N atoms black and Li ions gray (ellipsoids with a probability of 50%).

The Si–N distances in Li_2SiN_2 range between 1.724(2) and 1.790(2) Å, except Si1–N8 [1.820(2) Å] being slightly elongated. Nevertheless, the values are in the typical range for nitridosilicates.[26] The Li^+ ions are located between the two Si/N-sub-structures, resulting in a unique coordination sphere for each of the eight symmetrically independent Li^+ sites. The coordination spheres (cf. Figure 3) were assigned by lattice energy calculations (MAPLE; Madelung part of lattice energie).[27,28] Half of the Li^+ ions are four-coordinate by nitrogen atoms and three are five-coordinate. Li8 exhibits only three nitrogen contacts. According to the calculations, the next N-atom N2 [Li8–N2 2.790(6)] has no

significant contribution on the coordination sphere of Li8. This leads to the assumption, that the structure is dominated by the two interpenetrating $[Si_4N_6]N_{4/2}$ super-tetrahedron networks and the Li^+ ions have to be satisfied with a number of differing and uneven coordination spheres. This structural and electrostatic compromise might be responsible for the conversion of Li_2SiN_2 to $LiSi_2N_3$ at elevated temperatures or in an open reaction system.[22] $LiSi_2N_3$ adopts a highly ordered and electrostatically quite stable wurtzite-type structure with uniformly tetrahedrally coordinated Li^+ ions.[15]

Concerning the distances of neighboring Li^+-sites in Li_2SiN_2, there is a series of short Li–Li distances below 2.5 Å. These distances are visualized in Figure 3 (dashed lines). For comparison, the shortest Li–Li distance in $LiSi_2N_3$ is 2.92(1) Å.[15] The N-polyhedra around adjacent Li-sites featuring short Li–Li distances are additionally face- or at least edge-sharing. The combination of this fact and the uneven coordination spheres of the Li^+ ions might be responsible for the Li^+ ion conductivity observed at elevated temperatures.[21,22] By connecting Li1, Li2, Li3 and Li7 (Li4 and Li6: no short Li–Li contacts; Li5 and Li8 only one Li–Li contact, leading to a dead end) as illustrated in Figure 4, we assume possible Li pathways for Li ion conductivity. According to this assumption, the Li^+ ions could move in layers parallel to [001]. Admittedly, Li^+ ion conductivity results from complex interactions of structural features, defects, vacancies and can usually not only be explained on structural arguments.

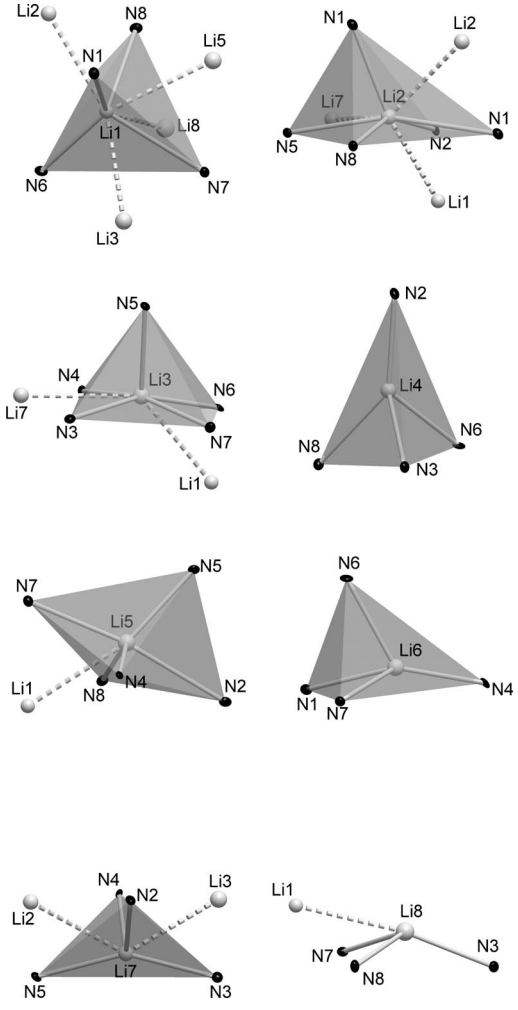

Figure 3. Coordination spheres of the eight crystallographically independent Li^+ ions in Li_2SiN_2 (ellipsoids with a probability of 50%).

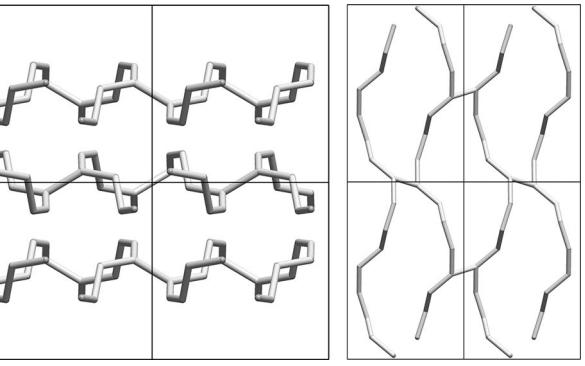

Figure 4. Illustration of possible channels constructed by short Li–Li distances, viewing direction along [001] left and [010] right. The Li1, Li2, Li3 and Li7 are connected by bonds printed in dark gray forming layers parallel [001].

Solid-State MAS NMR

During the last years, a series of nitridosilicates have been characterized using solid-state MAS NMR spectroscopy, resulting in a δ scale for ^{29}Si from –28 ppm observed for reduced nitridosilicates ($SrSi_6N_8$[26]) to oxo-nitridosilicates (–68 ppm, $Ba_3Si_6O_9N_4$[29]) on the other end. The chemical shifts of ^{29}Si in the case of $[SiN_4]$ tetrahedrons are usually found in the region between –40 to –60 ppm. The ^{29}Si MAS spectrum of Li_2SiN_2 is depicted in Figure 5. It consists of an unresolved signal in the range of 35–38 ppm. The four crystallographically independent Si atoms of Li_2SiN_2 are forming a highly symmetrical super-tetrahedron. Consequently, a conjunction of the ^{29}Si signals is consistent with the crystal structure. The low-field shift could possibly be caused by the high negative charge of the

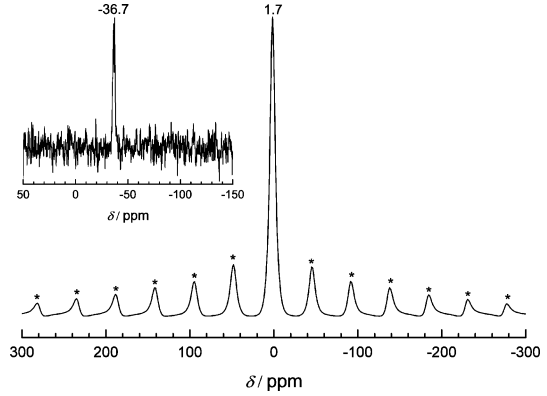

Figure 5. Solid-state MAS NMR spectra of ^7Li and ^{29}Si (inset). Rotation bands are indicated by stars (rotation frequency 9 kHz).

$[[Si_4N_6]N_{4/2}]^{8-}$ group and the surrounding Li^+. The ^7Li solid-state NMR spectrum of Li_2SiN_2 (Figure 5) consists of an intense isotropic peak centred at 1.7 ppm (FWHM: 1460 Hz, 7.5 ppm). The observed chemical shift value of 1.7 ppm is comparable to that of $LiSi_2N_3$ (δ = 1.3 ppm).[30] Due to the low resolution offered by ^7Li one can not distinguish between the eight crystallographically independent Li^+ ions.

Conclusions

The current investigation reveals that "$Si(CN_2)_2$" is an alternative precursor for $Si(NH)_2$ for the low-temperature synthesis of nitridosilicates. The reaction mechanism yielding nitridosilicates using "$Si(CN_2)_2$" differs from the mechanism suggested for $Si(NH)_2$ and can be described as metathesis. Meyer et al. recently pointed out the usefulness of metathesis reactions for the synthesis of new solid-state compounds.[31] Accordingly, we are confident to utilize "$Si(CN_2)_2$" as valuable precursor for a series of new nitridosilicates. Particularly, the reaction products exhibit good crystallinity. This has been shown by crystals of Li_2SiN_2 being suitable for single-crystal structure analysis. The crystal structure analysis reveals a unique $[[Si_4N_6]N_{4/2}]^{8-}$ network comprising differently coordinated Li^+ ions. On the basis of Li–Li distances and coordination polyhedrons possible Li^+ pathways are illustrated. Furthermore a phase pure synthesis for Li_2SiN_2 based on $Si(NH)_2$ has been developed and the solid-state MAS NMR spectroscopic data of ^7Li and ^{29}Si have been acquired.

Experimental Section

Synthesis: All manipulations were performed with rigorous exclusion of oxygen and moisture in flame-dried Schlenk-type glassware on a Schlenk line interfaced to a vacuum (10^{-3} mbar) line or in an argon-filled glovebox (Unilab, MBraun, Garching, $O_2 <$ 0.1 ppm, $H_2O <$ 0.1 ppm). Argon (Messer-Griessheim, 5.0) was purified by passage through columns of silica gel (Merck), molecular sieves (Fluka, 4 Å), KOH (Merck, ≥ 85%), P_4O_{10} (Roth, ≥ 99%, granulate) and titanium sponge (Johnson Matthey, 99.5%, grain size ≤ 0.8 cm) at 700 °C. "$Si(CN_2)_2$" was synthesized as described in the literature[12] and calcinated at 350 °C under vacuum (10^{-3} mbar) for 18 h. Li_3N was purchased from Alfa Aesar (99.4%) and $Si(NH)_2$ was synthesized according to the literature.[32]

For the synthesis of Li_2SiN_2 tantalum tubes (wall thickness 0.5 mm, internal diameter 10 mm, length 300 mm) were cleaned in a mixture of HNO_3 (conc.) and HF (40%). They were weld shut under a pressure of 1 bar purified Argon in an arc furnace. The crucible holder was water-cooled in order to avoid starting of the reaction during welding.

Single crystals of Li_2SiN_2 were synthesized from 32 mg of Li (4.6 mmol), 50 mg of "$Si(CN_2)_2$" (0.46 mmol) and 32 mg of Li_3N (0.92 mmol) in closed tantalum crucibles placed in silica tubes. The silica tube (under argon) was placed in the middle of a tube furnace. The temperature was raised to 900 °C (rate 120 °C h^{-1}), maintained for 24 h, subsequently cooled to 500 °C (rate 5 °C h^{-1}) and finally quenched to room temperature by switching off the furnace.

Phase pure bulk samples of Li_2SiN_2 for solid-state MAS NMR were synthesized from 100 mg of "$Si(NH)_2$" (1.72 mmol) and 40 mg of Li_3N (1.15 mmol). The welded tantalum tubes were placed into a water-cooled quartz reactor of a radio-frequency furnace (type IG 10/200 Hy, frequency: 200 kHz, max. electrical output: 12 kW, Hüttinger, Freiburg)[11] under argon atmosphere, the temperature was raised to 1200 °C within 7 h. After 24 h the temperature was decreased to 700 °C within 48 h and finally quenched to room temperature by switching off the furnace.

X-ray Diffraction: By inspection under a microscope integrated in a glove-box, colorless single crystals of the title compound were isolated from residual lithium and enclosed in glass capillaries. Single-crystal X-ray diffraction data were collected on a STOE IPDS diffractometer (Mo-K_α radiation). The program package SHELX97 was used for structure solution and refinement.[33] Further details of the crystal structure investigations can be obtained from the Fachinformationszentrum Karlsruhe, 76344 Eggenstein-Leopoldshafen, Germany (Fax: +49-7247-808-666; E-mail: crysdata@fiz-karlsruhe.de) on quoting the depository number CSD-420126 (Li_2SiN_2), the names of the authors and citation of the publication. Powder diffraction data were collected in Debye–Scherrer geometry on a STOE Stadi P powder diffractometer with Ge(111)-monochromatized Cu-$K_{\alpha1}$ radiation (λ = 1.5406 Å). High-temperature in situ X-ray diffractometry was performed on a STOE Stadi P powder diffractometer [Ge(111)-monochromated Mo-$K_{\alpha1}$ radiation, λ = 0.7104 Å] with an integrated furnace, using sealed silica capillaries (Ø 0.5 mm) as sample containers. The samples were heated from 25 °C to 750 °C in steps of 50 °C, using a heating rate of 5 °C min^{-1}. There was some evidence for the formation of crystalline Li_2SiN_2 at 750 °C, but at these temperatures and above reactions with the silica tube occur as well. Thus, these findings are not discussed in detail.

Thermal Behaviour: DSC measurements between room temperature and 750 °C were conducted on a Mettler DSC 25 with a heating range of 5 °C min^{-1}. The only moderately pressure-resistant, closed copper crucible used as a sample container was placed in the calorimeter under an atmosphere of dry nitrogen. The reaction behavior was studied on mixtures of "$Si(NH)_2$" (3 equiv.) and Li_3N (2 equiv.) as well as "$Si(CN_2)_2$" (1 equiv.) and Li_3N (2 equiv.).

Solid-State MAS NMR: Experiments were performed at 11.74 T on a Bruker DSX 500 spectrometer equipped with a commercial 4 mm triple-resonance MAS probe at the ^{29}Si and ^7Li frequencies of 99.385 MHz and 194.399 MHz, respectively. All experiments were performed in ZrO_2 rotors at room temperature. The chemical shifts of ^{29}Si and ^7Li are reported using the frequency ratios published by IUPAC [δ scale relative to 1% tetramethylsilane (TMS) in $CDCl_3$].[34] The one-dimensional ^{29}Si NMR spectrum was acquired with a 90° pulse length of 2.5 µs, a recycle delay of 64000 s and at a sample spinning frequency of 9 kHz. The one-dimensional ^7Li NMR spectrum was acquired with a 90° pulse length of 2.0 µs, a recycle delay of 64 s and at a sample spinning frequency of 9 kHz.

Supporting Information (see also the footnote on the first page of this article): PXRD pattern of Li_2SiN_2 in comparison to the simulation from single crystal structure analysis.

Acknowledgments

We are indebted to the following people for conducting the physical measurements: Dr. Jörn Schmedt auf der Günne and Christian Minke (solid-state NMR), Dr. Oliver Oeckler and Thomas Miller (single-crystal X-ray diffractometry), Wolfgang Wünschheim (DSC

measurements) [all Department Chemie and Biochemie, Universität München (LMU)]. The authors gratefully acknowledge financial support from the Fonds der Chemischen Industrie (FCI) and the Deutsche Forschungsgemeinschaft (DFG).

[1] W. Schnick, *Angew. Chem.* **1993**, *105*, 846–858; *Angew. Chem. Int. Ed. Engl.* **1993**, *32*, 806–818.
[2] R.-J. Xie, N. Hirosaki, *Sci. Technol. Adv. Mater.* **2007**, *8*, 588–600.
[3] W. Schnick, *Int. J. Inorg. Mater.* **2001**, *3*, 1267–1272.
[4] W. Schnick, H. Huppertz, *Chem. Eur. J.* **1997**, *3*, 679–683.
[5] Y. Q. Li, G. deWith, H. T. Hintzen, *J. Solid State Chem.* **2008**, *181*, 515–524.
[6] R.-J. Xie, N. Hirosaki, N. Kimura, K. Sakuma, M. Mitomo, *Appl. Phys. Lett.* **2007**, *90*, 191101/1–191101/3.
[7] X. Piao, T. Horikawa, H. Hanzawa, K. Machida, *Appl. Phys. Lett.* **2006**, *88*, 161908/1–161908/3.
[8] R. Mueller-Mach, G. Mueller, M. R. Krames, H. A. Höppe, F. Stadler, W. Schnick, T. Juestel, P. Schmidt, *Phys. Status Solidi A* **2005**, *202*, 1727–1732.
[9] M. Yamada, T. Naitou, K. Izuno, H. Tamaki, Y. Murazaki, M. Kameshima, T. Mukai, *Jpn. J. Appl. Phys.* **2003**, *42*, L20–L23.
[10] H. A. Höppe, H. Lutz, P. Morys, W. Schnick, A. Seilmeier, *J. Phys. Chem. Solids* **2000**, *61*, 2001–2006.
[11] W. Schnick, H. Huppertz, R. Lauterbach, *J. Mater. Chem.* **1999**, *9*, 289–296.
[12] A. Greiner, R. Riedel, G. Miehe, W. Dreßler, H. Fueß, J. Bill, F. Aldinger, *Angew. Chem.* **1997**, *109*, 657–660; *Angew. Chem. Int. Ed. Engl.* **1997**, *36*, 603–606.
[13] E. Kroke, R. Riedel, A. Greiner, A. O. Gabriel, L. Ruwisch, J. Nicolich, P. Kroll, *Chem. Mater.* **1998**, *10*, 2964–2979.
[14] R. L. LaDuca, P. T. Wolczanski, *Inorg. Chem.* **1992**, *31*, 1311–1313.
[15] M. Orth, W. Schnick, *Z. Anorg. Allg. Chem.* **1999**, *625*, 1426–1428.
[16] J. Grins, Z. Shen, S. Esmaeilzadeh, *Silic. Ind.* **2004**, *69*, 9–13.
[17] M. S. Bhamra, D. J. Fray, *J. Mater. Sci.* **1995**, *30*, 5381–5388.
[18] H. Hillebrecht, J. Cruda, L. Schröder, H. G. von Schnering, *Z. Kristallogr. Suppl.* **1993**, *6*, 80.
[19] R. Juza, H. H. Weber, E. Meyer-Simon, *Z. Anorg. Allg. Chem.* **1953**, *273*, 48–64.
[20] J. Lang, J.-P. Charlot, *Rev. Chim. Miner.* **1970**, *7*, 121–131.
[21] H. Yamane, S. Kikkawa, M. Koizumi, *Solid State Ionics* **1987**, *25*, 183–191.
[22] A. J. Anderson, R. G. Blair, S. M. Hick, R. B. Kaner, *J. Mater. Chem.* **2006**, *16*, 1318–1322.
[23] A. T. Dadd, P. Hubberstay, *J. Chem. Soc., Dalton Trans.* **1982**, 2175–2179.
[24] W. Schnick, U. Berger, *Angew. Chem.* **1991**, *103*, 857–858; *Angew. Chem. Int. Ed. Engl.* **1991**, *30*, 830–831.
[25] Z. A. Gál, P. M. Mallinson, H. J. Orchard, S. J. Clarke, *Inorg. Chem.* **2004**, *43*, 3998–4006.
[26] F. Stadler, O. Oeckler, J. Senker, H. A. Höppe, P. Kroll, W. Schnick, *Angew. Chem.* **2005**, *117*, 573–576; *Angew. Chem. Int. Ed.* **2005**, *44*, 567–570.
[27] R. Hübbenthal, *Programm zur Berechnung des Madelunganteils der Gitterenergie*, version 4, University of Gießen, **1993**.
[28] R. D. Shannon, *Acta Crystallogr., Sect. A: Cryst. Found. Crystallogr.* **1976**, *32*, 751–767.
[29] F. Stadler, W. Schnick, *Z. Anorg. Allg. Chem.* **2006**, *632*, 949–954.
[30] P. Kempgens, R. K. Robin, D. P. Thompson, *Solid State Nucl. Magn. Reson.* **1999**, *15*, 109–118.
[31] J. Glaser, H.-J. Meyer, *Angew. Chem.* **2008**, *120*, 120–123; *Angew. Chem. Int. Ed.* **2008**, *47*, 7547–7550.
[32] H. Lange, G. Wötting, G. Winter, *Angew. Chem.* **1991**, *103*, 1606–1625; *Angew. Chem. Int. Ed. Engl.* **1991**, *30*, 1579–1597.
[33] G. M. Sheldrick, *SHELX97*, release 97–2, Program package for the solution and refinement of crystal structures, University of Göttingen, Germany, **1997**.
[34] R. K. Harris, E. D. Becker, S. M. Cabral de Menezes, R. Goodfellow, P. Granger, *Solid State Nucl. Magn. Reson.* **2002**, *22*, 458–483.

Received: December 1, 2008
Published Online: February 11, 2009

